OPTIMUM PROPELLERS REVISITED - BEYOND BLADE ELEMENT THEORY

S P Fiddes*, K Brown and P C Bunniss†
Department of Aerospace Engineering
University of Bristol
Bristol, United Kingdom

Abstract

A method for the analysis of propellers and the design of optimum propellers is described. The method is based on representing the rotor system and its wake by a set of line vortices. The wake may be relaxed to model the contraction of the wake. The method does not require the assumptions used in classical blade-element and momentum theory and is thus less restrictive. The vortex theory described here is used to verify some of the assumptions of blade-element theory. Application of the vortex method to the design of two propellers is described and the results compared with those of classical blade design methods. It is found that the results are in good agreement with the classical blade element theory, although the effect of the tip vortex is found to be quite marked at low advance ratios.

Introduction

As suggested by Lanchester in 1907[13], a propeller may be modelled aerodynamically by bound and trailing vortices, where the velocities induced by the trailing helical vortices at the blade modify the relative airflow there. Although expressions for these wake-induced velocities can be written down using the Biot-Savart law for vortex-induced velocities, the numerical evaluation of these expressions is in general not possible in a simple form. The calculation of the induced velocities is the most difficult aspect of the practical application of the vortex theory of propellers. In fact one of the earliest versions of blade-element theory due to Drzewiecki[5] ignored the induced velocities entirely and while there were a few attempts to compute it in Japan[12] and Russia (see the work of Joukowski referred in[2]), these approaches were quickly abandoned as a potential route to a practical calculation procedure with the available computing facilities of the time.

Various idealisations were used to simplify the problem with the greatest advances in propeller analysis methods following from the work of Prandtl and Glauert[7] where a combination of blade element and momentum theory was developed – in effect obviating the need to calculate the induced velocities of the vortex wake via a Biot-Savart expression. Subsequently, Goldstein[8] produced a theory for the velocities induced by an idealized vortex wake, refined by Lock[15] for practical application. The essential difference between the Prandtl/Glauert and Goldstein approaches is the means by which the wake induced velocities are calculated. However, they share common assumptions. Fundamental amongst these is the 'blade-independence principle'. Glauert[6] gives a qualitative description of why the wake–induced velocities at a particular radial station on the blade should depend on the loading at that station alone. Experimental investigations by Lock *et al*[16] have shown this to be a valid assumption for most parts of the blade. Another assumption is that the wake does not contract. This implies that the increase in axial velocity of the air passing through the propeller is small, i.e. the propeller is not producing a 'large' amount of thrust per unit area of the propeller disc and is lightly-loaded. This assumption was relaxed by Theodorsen[17], who introduced corrections to the basic theory to allow for highly loaded propellers. Finally, the velocities induced by the vortex system at the blade are assumed to be half the values induced in the wake far downstream. This result follows from considering the velocities induced by an infinite and semi-infinite helical vortex filament of fixed pitch and radius, (where this wake shape is a consequence of the lightly-loaded assumption.) These assumptions have been the cornerstones of classical blade–element theory for several decades yet little has been done to assess their accuracy or range of applicability.

Within the framework of lightly-loaded propellers, Betz[3] was able identify the optimum load distribution on a propeller – i.e. the propeller design requiring min-

*Senior Lecturer, Member AIAA
†Research Fellow, Member RAeS

imum power input to produce a given thrust. A similar study using the calculus of variations is reported in [11]

For completeness, a brief summary of blade-element theory as developed by Glauert is given in the next section. The results of this classical theory are compared with a new vortex theory later in the paper.

Blade-Element Theory

From the blade independence assumption, we can treat each radial station of the blade separately. Consider a propeller with B blades rotating with angular velocity ω in an axial flow of velocity V and examine the conditions at a radial distance r from the axis of rotation. We define the solidity, σ, by

$$\sigma = \frac{Bc}{2\pi r} \tag{1}$$

where c is the chord at r. The Prandtl tip correction factor is (see Glauert[7]);

$$F = \frac{2}{\pi}\cos^{-1} e^{-f} \tag{2}$$

where

$$f = \frac{B}{2}\frac{(1-\bar{r})}{\sin\phi_t} \tag{3}$$

where $\bar{r} = \frac{r}{R}$, R is the tip radius and ϕ_t is found from $R\tan\phi_t = r\tan\phi$, where R is the radius of the blade tip and ϕ is the angle between the local flow at the blade and the blade disc. The element of lift ($\mathrm{d}L$) and drag ($\mathrm{d}D$) acting on the blade element are given in terms of the lift and drag coefficient of the blade sections by

$$\begin{aligned} \mathrm{d}L &= C_L \tfrac{1}{2}\rho W^2 c\,\mathrm{d}r \\ \mathrm{d}D &= C_D \tfrac{1}{2}\rho W^2 c\,\mathrm{d}r \end{aligned} \tag{4}$$

where W is the total velocity at the blade element and may be found via

$$W = \frac{V(1+a)}{\sin\phi} = \frac{\omega r(1-b)}{\cos\phi} \tag{5}$$

Here a is the inflow factor and b is the swirl factor and represent the velocities induced by the trailing vortex system at the blade. From the assumptions of blade-element theory the corresponding values of the inflow and swirl factors in the far wake are twice those at the blade element.

It is more convenient to use the axial and circumferential force coefficients defined by:

$$\begin{aligned} C_Y &= C_L\cos\phi - C_D\sin\phi \\ C_X &= C_L\sin\phi + C_D\cos\phi \end{aligned} \tag{6}$$

The elemental contribution to the thrust on the blade element is

$$\mathrm{d}T = \underbrace{BC_Y \tfrac{1}{2}\rho W^2 c\mathrm{d}r}_{\text{Force on blade element}} = \underbrace{\rho V(1+a)2\pi r\mathrm{d}r 2VaF}_{\text{Momentum increase in far wake}} \tag{7}$$

where the force on the blade element is given in terms of the coefficient of thrust on the blade and also in terms of the momentum in the far wake. From these expressions we have

$$\frac{\sigma}{4}C_Y\left(\frac{W}{V}\right)^2 = \frac{\sigma}{4}C_Y\left(\frac{1+a}{\sin\phi}\right)^2 = (1+a)aF \tag{8}$$

thus

$$\frac{\sigma}{4}\frac{C_Y}{\sin^2\phi} = \sigma Y = \frac{a}{1+a}F \tag{9}$$

This may be solved to give the inflow factor as

$$a = \frac{\sigma Y}{F - \sigma Y} \tag{10}$$

Similarly, the contribution to the torque on the propeller acting on the blade element is;

$$\mathrm{d}Q = nC_X\tfrac{1}{2}\rho W^2 cr\mathrm{d}r = \rho V(1+a)2\pi r\mathrm{d}r 2\omega r b F r \tag{11}$$

where again two expressions are available, one in terms of the force on the blade and the other is the increase in angular momentum in the wake. From these we obtain:

$$\begin{aligned} &\frac{\sigma}{4}C_X\frac{W^2}{V\omega r} \\ &= \frac{\sigma}{4}C_X\left(\frac{(1+a)(1-b)}{\sin\phi\cos\phi}\right) \\ &= (1+a)bF \end{aligned} \tag{12}$$

which simplifies to

$$\frac{\sigma}{4}\frac{C_X}{\sin\phi\cos\phi} = \sigma X = \frac{b}{1-b}F \tag{13}$$

which in turn may be rearranged to give the swirl factor

$$b = \frac{\sigma X}{F + \sigma X} \tag{14}$$

The wake helix angle at the blade is given by;

$$\tan\phi = \frac{V(1+a)}{\omega r(1-b)} = \frac{V}{\omega R}\frac{R}{r}\frac{(1+a)}{(1-b)} \tag{15}$$

Defining $\lambda = \frac{V}{\omega R}$, $\bar{r} = \frac{r}{R}$ and substituting for a (equation 10), b (equation 14) and using equations 13 and 9 we obtain

$$\left(F\sin^2\phi - \frac{\sigma}{4}C_Y\right) = \frac{\lambda}{\bar{r}}\left(F\sin\phi\cos\phi + \frac{\sigma}{4}C_X\right) \tag{16}$$

This is the main equation used in this paper the iterative solution procedure for ϕ at each radial station on the blade.

Optimum Design

Consider the case of a drag-free section (i.e. only circulation is present on the blade) then

$$\begin{aligned} C_Y &= C_L \cos\phi \\ C_X &= C_L \sin\phi \end{aligned} \tag{17}$$

so equation16 becomes

$$\left(F\sin^2\phi - \frac{\sigma}{4}C_L\cos\phi\right) = \frac{\lambda}{\overline{r}}\left(F\sin\phi\cos\phi + \frac{\sigma}{4}C_L\sin\phi\right) \tag{18}$$

this may be re-arranged to give;

$$\frac{\sigma}{4}C_L = F\sin\phi\frac{\left(\sin\phi - \frac{\lambda}{\overline{r}}\cos\phi\right)}{\left(\cos\phi + \frac{\lambda}{\overline{r}}\sin\phi\right)} \tag{19}$$

where the left hand side is just a function of $\overline{r}$ and ϕ for a given λ. Betz[3] has shown that when a propeller carries the optimum load distribution the far wake rotates as a rigid screw surface. The optimization process is thus as follows. First a value is estimated for $\phi_{t\infty}$, the value of the tip wake helix angle far downstream. The optimum condition is that the helix angle for the wake far downstream obeys the following relationship;

$$r\tan\phi_\infty = \text{constant} = R\tan\phi_{t\infty} \tag{20}$$

or

$$\tan\phi_\infty = \frac{\tan\phi_{t\infty}}{\overline{r}} \tag{21}$$

with

$$\begin{aligned} \tan\phi_\infty &= \frac{V(1+2a)}{\omega r(1-2b)} \\ &= \frac{\lambda}{\overline{r}}\frac{1+2a}{1-2b} \end{aligned} \tag{22}$$

We have the earlier results;

$$a = \frac{\sigma Y}{F - \sigma Y} \tag{23}$$

with

$$\begin{aligned} \sigma Y &= \frac{\sigma C_Y}{4\sin^2\phi} \\ &= \frac{\sigma C_L}{4\sin\phi}\cot\phi \end{aligned} \tag{24}$$

substituting for σC_L from equation 19, we obtain;

$$a = \frac{\overline{r}}{\lambda}\cos\phi\left(\sin\phi - \frac{\lambda}{\overline{r}}\cos\phi\right) \tag{25}$$

Similarly, we may derive an expression for the swirl inflow factor, b,

$$b = \frac{\sigma X}{F + \sigma X} \tag{26}$$

as $C_X = C_L\sin\phi$ this leads to

$$b = \sin\phi\left(\sin\phi - \frac{\lambda}{\overline{r}}\cos\phi\right) \tag{27}$$

The helix angle of the far wake is given by

$$\begin{aligned} \tan\phi_\infty &= \frac{V(1+2a)}{\omega r(1-2b)} \\ &= \frac{\lambda}{\overline{r}}\frac{1+2a}{1-2b} \end{aligned} \tag{28}$$

Now, from equations 25 and 27;

$$\frac{1+2a}{1-2b} = \frac{1+2\frac{\overline{r}}{\lambda}\cos\phi\left(\sin\phi - \frac{\lambda}{\overline{r}}\cos\phi\right)}{1-2\sin\phi\left(\sin\phi - \frac{\lambda}{\overline{r}}\cos\phi\right)} \tag{29}$$

thus equation 28 becomes

$$\tan\phi_\infty = \frac{\lambda}{\overline{r}}\frac{\frac{\overline{r}}{\lambda}\tan 2\phi - 1}{\frac{\lambda}{\overline{r}}\tan 2\phi + 1} \tag{30}$$

For an optimum propeller, we have the condition that the far wake forms a rigid screw surface;

$$\begin{aligned} \tan\phi_\infty &= \frac{\tan\phi_{t\infty}}{\overline{r}} \\ &= \frac{\lambda}{\overline{r}}\frac{\frac{\overline{r}}{\lambda}\tan 2\phi - 1}{\frac{\lambda}{\overline{r}}\tan 2\phi + 1} \end{aligned} \tag{31}$$

So, far a given $\tan\phi_{t\infty}$, we have

$$\frac{\tan\phi_{t\infty}}{\lambda} = \frac{\frac{\bar{r}}{\lambda}\tan 2\phi - 1}{\frac{\lambda}{\bar{r}}\tan 2\phi + 1} \tag{32}$$

This may be re-arranged to give

$$\tan 2\phi = \frac{\frac{\tan\phi_{t\infty}}{\lambda} + 1}{\frac{\bar{r}}{\lambda} - \frac{\tan\phi_{t\infty}}{\bar{r}}} \tag{33}$$

Given a value of $\phi_{t\infty}$, the advance ratio and radial station, equation 33 gives the flow angle at the blade from which the inflow factors, circulation and local thrust and power coefficients can be found. By integrating the local power coefficient across the blade the total power coefficient is found and compared with the desired value. $\phi_{t\infty}$ is varied (via a Newton iteration) until the desired power coefficient is obtained.

After the development of blade–element theory there has been little further development in propeller theory. The optimum results of Betz (leading to the result shown above) have been used recently by Larrabee[14] and Adkins and Liebeck[1] to design and analysis modern for low-speed applications (including propeller for man-powered aircraft) with great success. Designs for higher speed applications are still based on the Goldstein/Lock theory, but with allowance for compressible flow over the blade sections.

To quote Larrabee[14] "*The next step up to a 'prescribed' or 'free' discrete vortex model of the 'rotor' and its 'wake' is much more difficult*".

Here we take this 'next step' and now describe the development of a new propeller theory based on the fundamental vortex description of a propeller and compare it with results from the classical and new theories.

A Line-Vortex Model for Rotor Flows

As a rotor system may be replaced by a bound vortex system and a set of trailing vortices forming a helical surface an inviscid calculation of the flow past the blades can then be obtained by a generalization of the lifting line theory for conventional wings. In particular, it is most convenient if an iterative procedure is used. If the circulation distribution across the blade is initially assumed, then the distribution of circulation in the wake follows from the Helmholtz law. The wake vorticity will induce velocities at the blade. These velocities may be found, in principle, from the Biot-Savart law if the wake shape is known and combined vectorially with the relative airflow at the blade due to forward speed and rotation, to give the total relative airspeed at each section of the blade and the angle of flow to the disc plane. This in turn implies (for a given blade pitch setting) an angle of attack which determines the blade lift coefficient and hence its circulation. This leads to a new estimate of the circulation distribution across the blade and so the iteration process can be repeated until a converged answer is obtained.

A numerical method for calculating the velocities induced by the semi-infinite helical trailing vortex filaments is used here. The present approach represents the wake in two parts - a near field and a far-field region. The vortex filaments in the near field region are replaced by a series of straight vortex filaments, following a helical path. The Biot-Savart law is then used to calculate the velocity induced by each vortex segment. An asymptotic expression is then used for the velocity induced by the remainder of the wake. An early version of the present method is described and applied to wind-turbine applications in Gould and Fiddes[10]. Gould[9] conducted a survey of a number of methods for estimating the influence of the far-wake, and found that the method proposed by Wood and Meyer[18] gave the most accurate results and was computationally efficient.

The near-field vortex filaments can be relaxed, to align themselves with the local flow direction. Each of the far-field vortex filaments is taken with fixed pitch and radius to downstream infinity. The pitch and radius of the far-field filaments is fixed by the pitch and radius of the last part of the adjoining near-field filament.

The lifting-line method has been investigated extensively by Brown[4] to assess its accuracy. The key numerical parameters are:

1 Number of trailing vortices per blade

2 Number of turns in near wake

3 Number of vortex segments per turn in near wake

4 Radial distribution of horseshoe vortices and control points

It is, of course, desirable to use the minimum number of vortex filaments to represent the wake while preserving the required degree of accuracy in the solution. To achieve such an efficient model of the wake it has been found desirable to use a 'cosine' distribution and

use 'horseshoe' vortices comprising adjacent wake filaments. Then it is found that ten horseshoe vortices per blade are sufficient to give good accuracy, with two turns being used for the 'near-field' part of the wake with each turn comprising 24 vortex segments. These values have been used for the remainder of this study.

Wake Relaxation

An important part of the calculation procedure, especially for highly-loaded propellers, is the relaxation of the trailing vortex wake so that it takes up a force-free position. This is carried out for the inner wake region, the semi-infinite part of the wake continuing with constant pitch and radius set by the last turn of the inner wake.

The wake is initially a prescribed one, following the 'lightly-loaded' direction of the rigid screw wake, i.e. following the air path traced by the blade. For a given loading on the blade, the velocities induced in the near-field wake are computed and the line vortex segments aligned with the local flow. This is performed by 'sweeping' downstream with relaxation being applied in successive downstream planes. A number of downstream sweeps are performed during each relaxation cycle.

During the relaxation some vortices approach one another closely and can develop large variations in position from sweep to sweep. To alleviate this problem, a vortex-merging procedure is used where vortices are combined if they approach within a given distance of each other. This has been found to be very effective in stabilizing the wake roll-up process.

Thrust and Power Coefficients

Using the method described above for computing the wake induced velocities for a given wake (which may be a relaxed wake), we may write;

$$u_i = \sum_j a_{ij}\Gamma_j \tag{34}$$

$$v_i = \sum_j b_{ij}\Gamma_j \tag{35}$$

where u_i is the axial velocity induced by the trailing wake system at collocation point i on the blade and v_i is the circumferential (or swirl) velocity. Thus a_{ij} is the contribution to u_i from the horseshoe vortex associated with radial position j. The a_{ij} and b_{ij} depend on the wake geometry, and may be computed once the wake shape is obtained, either via a prescribed or relaxed wake solution.

From the Kutta relationship for the force on the bound vortex representing the blade, and ignoring the profile drag of the blade sections, we can write for the total torque (Q) and thrust (T) on the blade;

$$T = \rho \sum_i \Delta r_i(\omega r_i + v_i)\Gamma_i$$

$$Q = \rho \sum_i r_i \Delta r_i(V + u_i)\Gamma_i$$

Where r_i is the "average" radial position of horseshoe vortex i (taken as the collocation point) and Δr_i is the length of the bound portion of that vortex. The power, P, is related to the torque via $P = Q\omega$

The following non-dimensionalisation is now introduced: all lengths are non–dimensionalised with respect to the tip radius R, and all velocities are nondimensionalised with respect to the rotational tip speed, ωR (hence the circulations are nondimensionalised by ωR^2). Furthermore, it is convenient to express the thrust and power in coefficient form and use the advance ratio instead of the forward speed, i.e.

$$C_T = \frac{T}{\rho n^2 D^4} = \frac{B\pi^2}{4} \sum_i \Delta r_i(r_i + v_i)\Gamma_i \tag{36}$$

$$C_P = \frac{P}{\rho n^3 D^5} = \frac{B\pi^3}{4} \sum_i r_i \Delta r_i \left(\frac{J}{\pi} + u_i\right)\Gamma_i \tag{37}$$

where, J is the advance ratio ($J = \dfrac{V}{nD} = \dfrac{\pi V}{\omega R}$), D is the diameter of the blades ($= 2R$), n is the revolutions per second ($= \dfrac{\omega}{2\pi}$) and the other symbols now represent non-dimensional values.

Optimum Propellers

The optimization problem is now introduced: given a propeller with B blades each of radius R, operating at an advance ratio J with a power coefficient C_{P_o}, what is the maximum thrust coefficient that can be produced and what form of load (or circulation) distribution across the blade gives this maximum thrust?

To answer this question we maximize the following expression with respect to the Γ_i's;

$$L(\Gamma, \lambda) = C_T + \lambda(C_{P_o} - C_P) \tag{38}$$

where Γ is the vector of Γ_i's and λ is a Lagrange multiplier.

To obtain an extremal value of the function L, we must have $\frac{\partial L(\Gamma,\lambda)}{\partial \Gamma_k} = 0$ for each value of k. This is found via:

$$\begin{aligned}\frac{\partial C_T}{\partial \Gamma_k} &= \frac{B\pi^2}{4}\sum_i \Delta r_i (r_i + v_i)\frac{\partial \Gamma_i}{\partial \Gamma_k} \\ &+ \frac{B\pi^2}{4}\sum_i \Delta r_i \frac{\partial v_i}{\partial \Gamma_k}\Gamma_i \qquad (39)\end{aligned}$$

Using the result $\frac{\partial \Gamma_i}{\partial \Gamma_k} = \delta_{ik}$, (the Kronecker delta) and

$$\begin{aligned}\frac{\partial v_i}{\partial \Gamma_k} &= \frac{\partial \sum_j b_{ij}\Gamma_j}{\partial \Gamma_k} \\ &= \sum_j b_{ij}\frac{\partial \Gamma_j}{\partial \Gamma_k} = b_{ik} \qquad (40)\end{aligned}$$

we have:

$$\begin{aligned}\frac{\partial C_T}{\partial \Gamma_k} &= \frac{B\pi^2}{4}\Delta r_k (r_k + v_k) \\ &+ \frac{B\pi^2}{4}\sum_i \Delta r_i b_{ik}\Gamma_i \qquad (41)\end{aligned}$$

The above equation represents two physical effects. The first term $(\frac{B\pi^2}{4}\Delta r_k(r_k + v_k))$ is the change in thrust on a given horseshoe vortex due to the change in strength of that vortex– this is a 'local' effect. The second term $(\frac{B\pi^2}{4}\sum_i \Delta r_i(r_i + b_{ik})\Gamma_i)$ is the effect due to the change velocity at all bound segments due to a change in circulation on one bound segment – this is a 'global' effect.

Similarly, we have for the rate of change of power with local vortex strength;

$$\begin{aligned}\frac{\partial C_P}{\partial \Gamma_k} &= \frac{B\pi^3}{4}\sum_i r_i \Delta r_i \left(\frac{J}{\pi} + u_i\right)\frac{\partial \Gamma_i}{\partial \Gamma_j} \\ &+ \frac{B\pi^3}{4}\sum_i r_i \Delta r_i \frac{\partial u_i}{\partial \Gamma_k}\Gamma_i \\ &= \frac{B\pi^3}{4} r_k \Delta r_k \left(\frac{J}{\pi} + u_k\right) \\ &+ \frac{B\pi^3}{4}\sum_i r_i \Delta r_i a_{ik}\Gamma_i \qquad (42)\end{aligned}$$

This again is made up of two terms - the 'local' effect and the 'global' effect.

The condition for an extremum is then

$$\begin{aligned}&\Delta r_k (r_k + v_k) + \sum_i \Delta r_i b_{ik}\Gamma_i \\ &- \lambda\pi\left(\sum_k r_k \Delta r_k \left(\frac{J}{\pi} + u_k\right) + \sum_i r_i \Delta r_i a_{ik}\Gamma_i\right) \\ &= 0 \qquad (43)\end{aligned}$$

for each k.

One result follows immediately from λ being the same value for all values of k, i.e. at each radial position we require that the ratio;

$$\frac{\Delta r_k (r_k + v_k) + \sum_i \Delta r_i b_{ik}\Gamma_i}{r_k \Delta r_k \left(\frac{J}{\pi} + u_k\right) + \sum_i r_i \Delta r_i a_{ik}\Gamma_i} = \lambda\pi \qquad (44)$$

is constant across the blade. Substituting for v_k and u_k in terms of the influence functions, we have;

$$\frac{\Delta r_k (r_k + \sum_i b_{ki}\Gamma_i) + \sum_i \Delta r_i b_{ik}\Gamma_i}{r_k \Delta r_k \left(\frac{J}{\pi} + \sum_i a_{ki}\Gamma_i\right) + \sum_i r_i \Delta r_i a_{ik}\Gamma_i} = \lambda\pi$$

or

$$\frac{\Delta r_k r_k + \sum_i (\Delta r_k b_{ki} + \Delta r_i b_{ik})\Gamma_i}{r_k \Delta r_k \frac{J}{\pi} + \sum_i (r_k \Delta r_k a_{ki} + r_i \Delta r_i a_{ik})\Gamma_i} = \lambda\pi \qquad (45)$$

Classical Propeller Theory Result

A link between the present analysis and the classical result of Betz for optimum propellers is now seen, if we make the same assumptions as used by Betz[3] in deriving his result for the optimum load distribution, viz:

(1) That the wake induced perturbation velocities at a given radial station depend only on the load carried at that station.

(2) That there is no wake contraction and the wake-induced perturbation velocities in the ultimate wake are twice those at the blade at the same radial station.

The first assumption implies that only the "diagonal terms" a_{ii} and b_{ii} are non-zero and the equation for the Lagrange multiplier becomes (reverting to dimensional quantities)

$$\begin{aligned}\pi\lambda &= \frac{\Delta r_k \omega r_k + (\Delta r_k b_{kk} + \Delta r_k b_{kk})\Gamma_k}{r_k \Delta r_k U + (r_k \Delta r_k a_{kk} + r_k \Delta r_k a_{kk})\Gamma_k} \\ &= \frac{\omega r_k + 2 b_{kk}\Gamma_k}{r_k (U + 2 a_{kk}\Gamma_k)} \end{aligned} \quad (46)$$

is a constant across the blade. From the assumptions above, $\omega r_k + 2b_{kk}\Gamma_k$ is the circumferential (or swirl) component of velocity in the far wake, while $U + 2a_{kk}\Gamma_k$ is the axial velocity there. The wake is aligned with these velocities, so the helix angle (ϕ) of the far wake is

$$\tan\phi_k = \frac{\omega r_k + 2 b_{kk}\Gamma_k}{U + 2 a_{kk}\Gamma_k} = \text{constant} \times r_k \quad (47)$$

from the optimality condition. The tangent of the helix angle of the far wake is thus proportional to the radial distance to each part of the wake. This implies the wake forms a rigid screw surface, in accordance with the Betz result.

Blade Independence?

The availability of a method for the accurate calculation the influence coefficients allows us to assess the assumption of independence of blade sections across the blade. The consequence of the independence of blade elements (if it is true in each case) is that the influence matrices calculated by the present method are diagonal, *i.e.* only the element a_{ii}, b_{ii} and c_{ii} are non-zero. A weaker requirement is that the influence matrices should be strongly diagonally dominant. Influence matrices corresponding to a range of conditions (different wake helix angles, number of blades), have been examined and a typical plot of the magnitude of the circumferential (swirl) influence matrix elements b_{ij} for two cases is shown in figures 1 and 2 for unrelaxed, prescribed wakes following the lightly-loaded wake shape. The plots show the logarithm of the magnitude of the influence coefficients, with the tip at the upper part of the figure and the hub at the lower. In each case the wake has been modelled by seventeen trailing vortices per blade.

The first is for a case with six blades at an advance ratio of $J = 0.39$. Here successive turns of the wake are in close proximity and the trailing vortex system is well-presented by a set of vortex cylinders, a case that should be well-represented by the blade-element theory. It is seen that the influence matrix is indeed strongly diagonally dominant.

The second example is for a two-bladed propeller at the same advance ratio. Figure 2 shows that the off-diagonal entries do not decrease in magnitude as rapidly as before, but the matrix is still diagonally dominant.

The assumption of blade independence is thus seen to be a good one, as studies of other influence matrices for a wide range of flow conditions show.

Solution of the Optimization Problem

For an assumed value of the Lagrange multiplier λ, equation45 gives a set of linear equations that may be solved for the circulations Γ.

$$\begin{aligned} &\Delta r_k r_k + \sum_i (\Delta r_k b_{ki} + \Delta r_i b_{ik})\Gamma_i \\ &- \lambda\pi \left(r_k \Delta r_k \frac{J}{\pi} + \sum_i (r_k \Delta r_k a_{ki} + r_i \Delta r_i a_{ik})\Gamma_i \right) \\ &= 0 \end{aligned} \quad (48)$$

Rearranging this expression, we have for each station k

$$\sum_i ((\Delta r_k b_{ki} + \Delta r_i b_{ik}) - \lambda\pi(r_k \Delta r_k a_{ki} + r_i \Delta r_i a_{ik}))\Gamma_i = (1 - \lambda J)\Delta r_k r_k \quad (49)$$

If λ is prescribed, equation 49 may be solved to give the Γ_i's. The power produced by this set of Γ_i's may be found from equation 37. This will, in general, differ from the prescribed power, so an iteration is performed with λ to find the value of the Lagrange multiplier that gives the specified power. A Newton iteration scheme is used in this paper. Once the value of λ giving the specified power has been found, the optimum Γ_i distribution and the thrust coefficient may be determined.

The loading optimization procedure is carried out for fixed wake geometry. When the optimum loading has

been found, the wake is relaxed, so that it is consistent with the most recent load distribution. Typically two to four relaxations are performed for a fixed circulation distribution. The relaxation will in general alter the shape of the wake and hence the influence functions. The optimization process then needs to be repeated for the new wake shape. This process is repeated until the loading does not change between two successive wake relaxations and optimizations.

Application Examples

Some examples of the application of the classical and new theory are now described. The first example is the design of a three-bladed propeller for a microlight aircraft. The design specification is the maximum thrust for conditions corresponding to an advance ratio of 0.433 and a power coefficient of 0.06. The classical (blade element) optimization of the design predicts a thrust coefficient of 0.106. Figure 3 shows the convergence of the circulation distribution with successive iterations for the vortex theory, while figure 4 compares the classical and vortex-theory predictions of optimum load distribution. The agreement is quite close, although the vortex theory has a marked nonuniformity near the tip. This is due to the effect of the tip vortex from the preceding blade that runs inboard of the blade due to the wake contraction. This leads to an unloading of the tip. Figure 5 shows the variation of predicted thrust coefficient with wake relaxation. It is noted that the vortex theory result approaches the classical result very closely. Figure 6 shows the unrelaxed and final relaxed wake shape for one blade. Note that for the relaxed wake the wake pitch increases downstream (due to the progressive increase in axial velocity in the wake) and the wake contracts, so that the actual wake shape is quite different from the lightly-loaded form. Nevertheless , the optimum classical design is quite close to the vortex-theory result. This agreement between classical and 'fuller' vortex theory for this case may be expected as the design condition is a lightly-loaded one at low advance ratios – conditions conducive to the the assumptions of blade-element theory being valid. However, the effect of the strong tip vortex on the outboard loading is not accounted for in the classical theory.

As the lightly-loaded example discussed above does not reveal any marked difference in the optimum design as predicted by blade-element and vortex theory, a more highly-loaded example is considered next. This is drawn from a six-bladed propeller design for a high-speed civil airliner with higher loading and advance ratio (a power coefficient of 1.0 and an advance ratio of 3.0).

Figure 7 shows the convergence history of the circulation distribution for ten wake relaxation cycles. Note there is hardly any change in optimum loading with wake relaxation. Figure 8 compares the classical and vortex-theory results – again the agreement is very good, perhaps surprisingly so in view of the design conditions. Figure 9 shows the convergence of the thrust coefficient with wake relaxation. Again the result is close to the classical method prediction in terms of thrust levels.

Figure 10 compares the unrelaxed and relaxed wake. The wake relaxation affects the downstream shape of the wake more strongly than the 'near wake'. The high advance ratio means that the wake is carried away from the blade quite quickly before rollup can alter the wake shape near the blade significantly and thus explains why the optimum loading does not change greatly with wake relaxation in figure 7.

Again, the classical and vortex theory results are very similar, perhaps more so than in the previous design example, as the tip vortex is swept downstream before approaching the following blade in the high speed case.

Conclusions

A new model for the flow past a propeller has been presented and a method for determining optimum designs in this new framework has been described. Comparison of the results of the new method with classical (blade-element) design procedures has strengthened some of the assumptions of the classical theory and given good agreement with 'classical optimum designs'. Perhaps surprisingly, the greatest discrepancies occur at low advance ratios, due to the proximity of the strong tip vortex from the preceding blade to the inboard section of the following blade. At high advance ratios the classical theory and vortex theory are in closer agreement.

References

[1] C N Adkins and R H Liebeck. Design of optimum propellers. AIAA Paper 83 - 0190, 1983.

[2] V E Baskin, L S Vil'dgrube, Ye S Vozhdayev, and G I Maykapar. Teoriya nesushcjego vinta. Translated as Theory of the Lifting Airscrew, NASA TT F-823, 1973.

[3] A Betz. Schraubenpropeller mit geringsten energieverlust. Göttinger Nachr., 1919.

[4] K Brown. Assessment of a nonlinear lifting-line method for rotor flows. University of Bristol, Dept of Aerospace Eng. Rpt., 1994.

[5] S K Drzewiecki. *Théorie Général de l'Helice Propulsive.* Gauthier–Villars (Paris), 1920.

[6] H Glauert. *Elements of Aerofoil and Airscrew Theory.* Cambridge University Press, 1926.

[7] H Glauert. Airplane propellers Division L, vol iv. In *Aerodynamic Theory (ed. Durand)*, pages 169 – 269. Julius Springer, 1935.

[8] S Goldstein. On the vortex theory of screw propellers. *Proc Roy. Soc. A*, 123:440 – 465, 1929.

[9] J Gould. *Computational Performance Prediction Methods for Horizontal Axis Wind Turbines.* PhD thesis, Department of Aerospace Engineering, University of Bristol, 1993.

[10] J Gould and S P Fiddes. Computational methods for the performance prediction of HAWTs. *Journal of Wind Engineering and Industrial Aerodynamics*, 39:61 – 72, 1992.

[11] A B Haines and K V Diprose. The application of the calculus of variations to propeller design with particular reference to Spitfire VII with Merlin 61 engine. ARC R&M No. 2083, 1943.

[12] S Kawada. Tokyo Imperial University, Aero. Res. Inst. Report No. 14, 1926.

[13] F W Lanchester. *Aerodynamics.* Constable & Co. (London), 1907.

[14] E E Larrabee. The design of propellers for motor-soarers. NASA Conference Proceedings 2085, Part 1, pgs 285 – 303, 1979.

[15] C N H Lock. Application of Goldstein's theory to the practical design of airscrews. ARC R&M No. 1377, 1930.

[16] C N H Lock, H Bateman, and H C H Townend. Experiments to verify the independence of the elements of an airscrew blade. ARC R&M No. 953, 1924.

[17] T Theodorsen. *Theory of Propellers.* McGraw-Hill Book Company Inc, 1948.

[18] D H Wood and C Meyer. Two methods for calculating the velocities induced by a constant diameter far wake. *Journal of Aircraft*, 28:526 – 531, 1991.

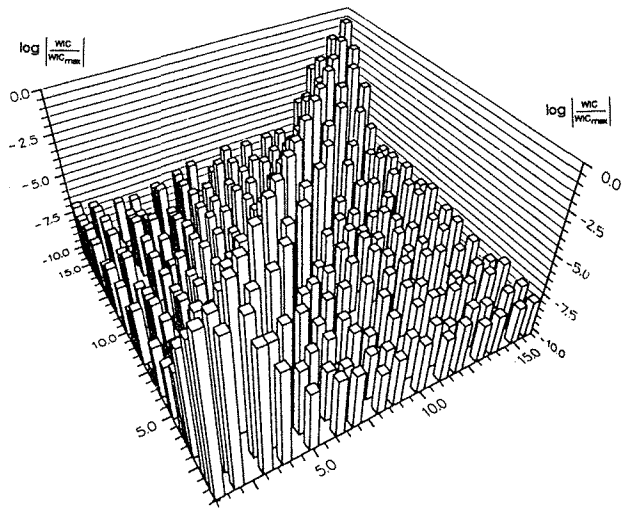

FIGURE 1
Influence Matrix

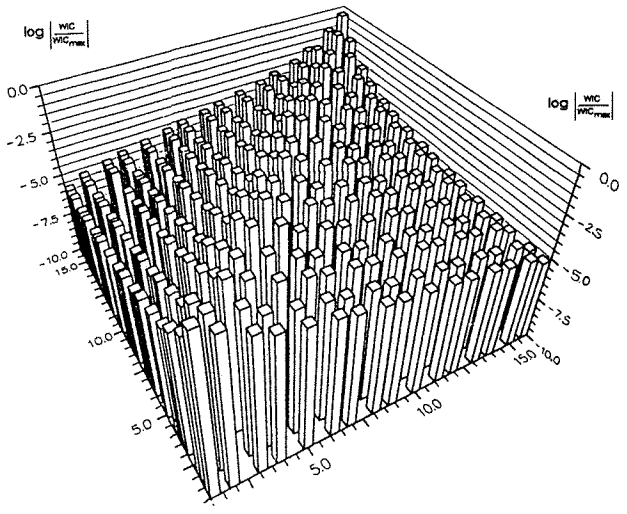

FIGURE 2
Influence Matrix

CIRCULATION DISTRIBUTION
Convergence with Wake Relaxations

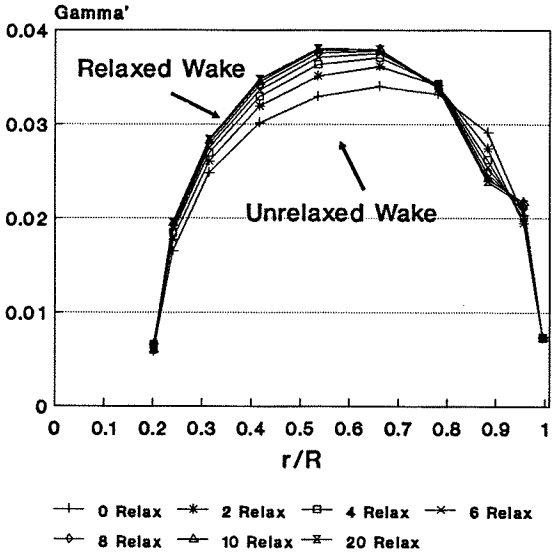

FIGURE 3

THRUST COEFFICIENT
Convergence with number of Wake Relaxations

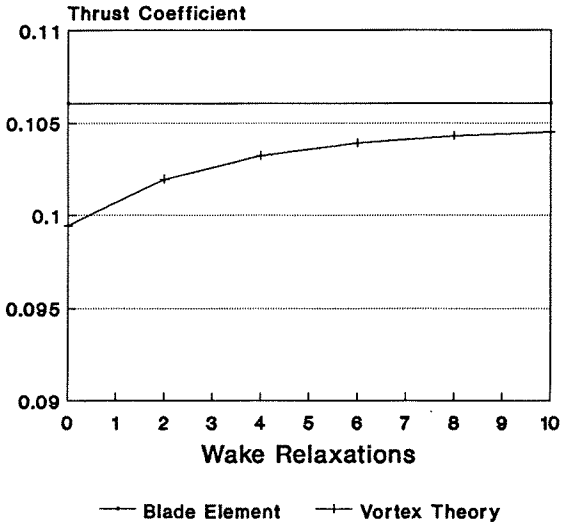

J = 0.433
Cp = 0.063112
FIGURE 5

CIRCULATION DISTRIBUTION
Comparison of Blade Element and Vortex Theory Optima

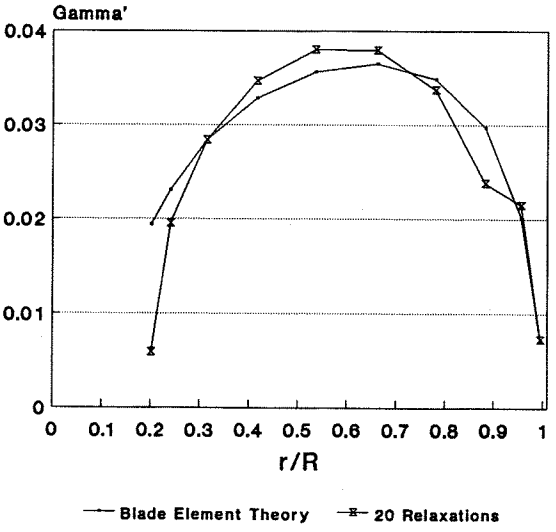

FIGURE 4

ORIGINAL AND RELAXED WAKES

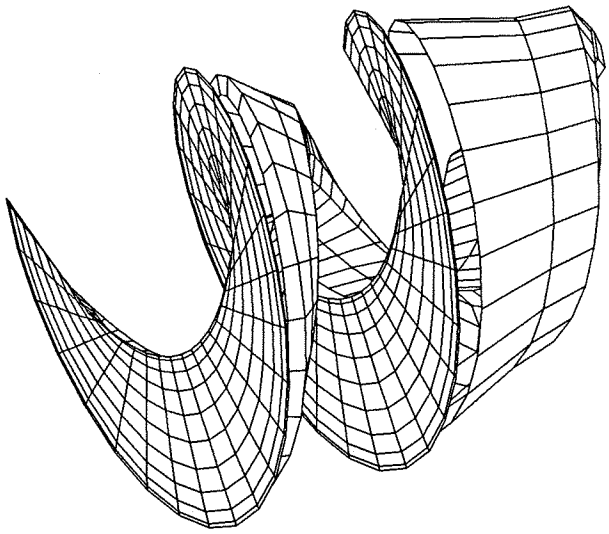

FIGURE 6

CIRCULATION DISTRIBUTION
Convergence with
Wake Relaxations

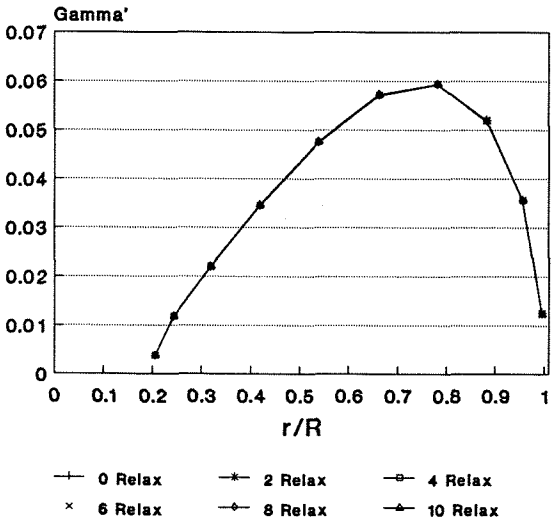

FIGURE 7

THRUST COEFFICIENT
Convergence with number
of Wake Relaxations

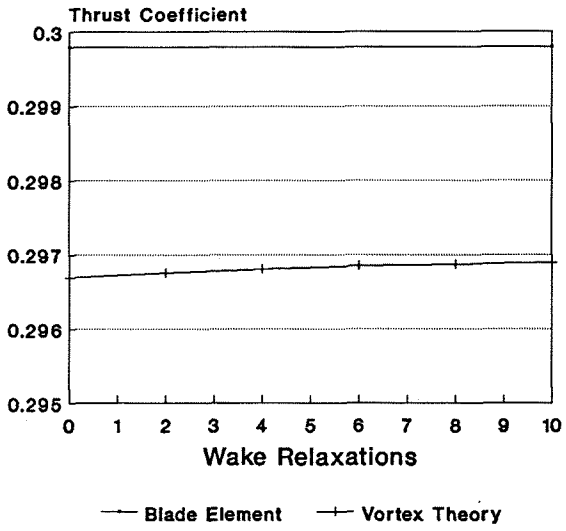

J = 3.0
Cp = 1.0

FIGURE 9

CIRCULATION DISTRIBUTION
Comparison of Blade Element
and Vortex Theory Optima

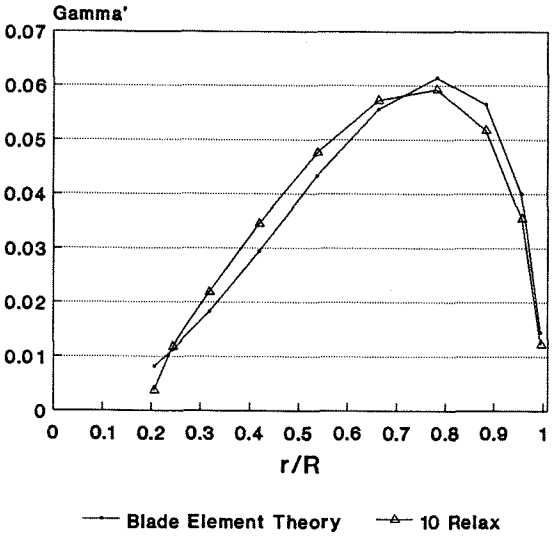

FIGURE 8

ORIGINAL AND
RELAXED WAKES

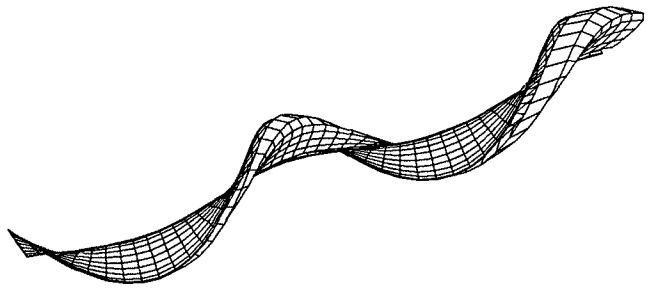

FIGURE 10